

Relativistic hydrodynamics for heavy-ion collisions

This article has been downloaded from IOPscience. Please scroll down to see the full text article.

2008 Eur. J. Phys. 29 275

(<http://iopscience.iop.org/0143-0807/29/2/010>)

[The Table of Contents](#) and [more related content](#) is available

Download details:

IP Address: 132.166.22.147

The article was downloaded on 09/04/2010 at 17:04

Please note that [terms and conditions apply](#).

Relativistic hydrodynamics for heavy-ion collisions

Jean-Yves Ollitrault

Institut de Physique Théorique, CEA/DSM/IPhT, CNRS/MPPU/URA2306 CEA Saclay,
F-91191 Gif-sur-Yvette Cedex, France

E-mail: jean-yves.ollitrault@cea.fr

Received 20 August 2007, in final form 4 January 2008

Published 28 January 2008

Online at stacks.iop.org/EJP/29/275

Abstract

Relativistic hydrodynamics is essential to our current understanding of nucleus–nucleus collisions at ultrarelativistic energies (current experiments at the Relativistic Heavy Ion Collider, forthcoming experiments at the CERN Large Hadron Collider). This is an introduction to relativistic hydrodynamics for graduate students. It includes a detailed derivation of the equations and a description of the hydrodynamical evolution of a heavy-ion collision. Some knowledge of thermodynamics and special relativity is assumed.

(Some figures in this article are in colour only in the electronic version)

1. Introduction

The use of relativistic hydrodynamics in the context of high-energy physics dates back to Landau [1], long before quantum chromodynamics (QCD) was discovered. High-energy collisions produce many hadrons of different sorts going into all directions. One expected that tools from statistical physics would shed light on this complexity. The light eventually came from the deep-inelastic scattering of electrons, which led to the parton model, and hydrodynamics was of little use. It is only in recent years, with the advent of heavy-ion experiments at the Relativistic Heavy Ion Collider (RHIC), that the interest in relativistic hydrodynamics has been revived. One of the first RHIC papers [2] reported on the ‘observation of a higher degree of thermalization than at lower collision energies’. Several phenomena were observed which suggested that the matter produced in these collisions behaves, collectively, like a fluid. It was even claimed in 2005 that the RHIC experiments had created a ‘perfect liquid’, with the lowest possible viscosity.

Relativistic hydrodynamics is interesting because it is simple and general. It is simple because the information on the system is encoded in its thermodynamic properties, i.e., its equation of state. Hydrodynamics is also general, in the sense that it relies on only one assumption, unfortunately a very strong one: local thermodynamic equilibrium. No other

assumption is made concerning the nature of the particles and fields, their interactions, the classical/quantum nature of the phenomena involved.

This paper is an introduction to relativistic hydrodynamics in relation with heavy-ion collisions. Relativistic hydrodynamics per se is textbook material since Landau's course has appeared (see chapter XV of [3]). As for its applications to heavy-ion collisions, they are covered by several recent reviews [4–6]. The recent experimental achievements show us the old textbook results under a new perspective, since it appears possible to produce a relativistic fluid in the laboratory. My purpose is to provide graduate students with an elementary, self-contained survey of this exciting research field. Section 2 recalls basic results of thermodynamics and statistical physics which are commonly used in the context of hydrodynamics. Section 3 derives the equations of inviscid hydrodynamics. Section 4 describes the hydrodynamical evolution of a heavy-ion collision; the details may be skipped upon first reading. Section 5 derives some observables which are used as signatures of hydrodynamical behaviour. Finally, section 6 briefly describes the domain of validity of hydrodynamics. The readers who are interested in relativistic hydrodynamics in itself should try and work out the problems given in the appendix.

2. Thermodynamics

We first recall standard identities of thermodynamics and statistical physics, which are often used in hydrodynamical models.

2.1. General identities

The differential of internal energy is given by the thermodynamic identity

$$dU = -P dV + T dS + \mu dN, \quad (1)$$

where P is the pressure, V is the volume, S is the entropy, T is the temperature and μ is the chemical potential. In nonrelativistic systems, N is generally the number of particles, which is conserved. In a relativistic system, the number of particles is not conserved: it is always possible to create a particle–antiparticle pair, provided energy is available. In this case, N no longer denotes a number of particles, but a conserved quantity, such as the baryon number. If there are several conserved quantities N_i , one needs to simply replace μdN with $\sum_i \mu_i dN_i$. In this paper, we refer to N as to the baryon number, and to μ as the baryon chemical potential, but N can be any conserved quantity. The second important difference in relativistic systems is that the mass energy mc^2 is included in the internal energy.

The first two terms on the right-hand side of (1) have transparent physical interpretations as the elementary work and heat transferred to the system, respectively. The third term is mathematically as simple as the two first terms, but lacks such a simple interpretation¹.

The energy is an extensive function of the extensive variables V , S , N , which means that

$$U(\lambda V, \lambda S, \lambda N) = \lambda U(V, S, N). \quad (2)$$

Differentiating with respect to λ , taking $\lambda = 1$, and using (1), one obtains

$$U = -PV + TS + \mu N. \quad (3)$$

¹ It does in fact have a simple interpretation in the more complex situation where a particle is exchanged between two different systems, e.g., between two solutions with different concentrations at the same pressure and temperature, as occurs in chemistry. It then plays the role of a thermodynamic potential, in the sense that it chooses the lowest possible value.

Differentiating this equation and using again (1), one obtains the Gibbs–Duhem relation

$$V dP = S dT + N d\mu. \quad (4)$$

In hydrodynamics, the useful quantities are not the total energy, entropy and baryon number, but rather their densities per unit volume, the energy density $\epsilon \equiv U/V$, the entropy density $s \equiv S/V$ and the baryon density $n \equiv N/V$. All these densities are intensive quantities. (3) and (4) give, respectively,

$$\epsilon = -P + Ts + \mu n \quad (5)$$

and

$$dP = s dT + n d\mu \quad (6)$$

Differentiating (5) and using (6), one obtains

$$d\epsilon = T ds + \mu dn. \quad (7)$$

These identities will be used extensively below.

2.2. Baryonless fluid

If the baryon density n vanishes throughout the fluid, the corresponding terms disappear from (5) to (7). The same holds if the chemical potential μ is zero throughout the fluid. This shows that ‘zero baryon density’ is in practice equivalent to ‘no conserved baryon number’. Such a fluid has only one intensive degree of freedom.

The fluid produced in a heavy-ion collision has three conserved charges, which are the net number of quarks (i.e., number of quarks minus number of antiquarks) of each flavour u, d, s . There is an excess of u and d quarks over antiquarks because of the incoming nuclei. However, this excess turns out to be negligible at ultrarelativistic energies because the number of produced particles overwhelms the number of incoming nucleons. In practice, doing a hydro calculation with $n = 0$ is a rough approximation, but a reasonable one.

2.3. Isentropic process

The entropy of an inviscid fluid is conserved throughout its evolution, as we shall see in section 3. This is why isentropic processes are important. In an isentropic process, both S and N are conserved, and only the volume V changes. The variations of entropy density and baryon density are given by

$$\frac{ds}{s} = \frac{dn}{n} = -\frac{dV}{V}. \quad (8)$$

To compute the variation of energy density, we use (1), which reduces to $dU = -P dV$:

$$dU = d(\epsilon V) = \epsilon dV + V d\epsilon = -P dV, \quad (9)$$

hence

$$\frac{d\epsilon}{\epsilon + P} = -\frac{dV}{V} = \frac{ds}{s} = \frac{dn}{n}. \quad (10)$$

2.4. Classical ideal gas

An ideal gas is made of independent particles, and is best described by the grand-canonical ensemble of statistical mechanics. We choose the natural system of units $k_B = 1$ (one recovers the conventional unit system by replacing everywhere $T \rightarrow k_B T$ and $S \rightarrow S/k_B$ in the expressions below). For simplicity, we consider a gas made of identical, spinless particles, each of which carries a baryon number equal to unity (although such particles do not exist).

In a finite volume V , the values of the momentum \vec{p} are discrete (from quantum mechanics). The average number of particles with momentum \vec{p} is $1/(\exp((E_{\vec{p}} - \mu)/T) \pm 1)$, where $E_{\vec{p}} \equiv \sqrt{\vec{p}^2 + m^2}$ is the particle energy (we choose the natural unit system where $c = 1$), and the sign depends on whether the particle is a fermion or a boson. For the sake of simplicity, we take the classical limit where this number is much smaller than unity: both Bose–Einstein and Fermi–Dirac statistics then reduce to Maxwell–Boltzmann statistics:

$$\frac{1}{e^{(E_{\vec{p}} - \mu)/T} \pm 1} \simeq e^{(-E_{\vec{p}} + \mu)/T} \ll 1. \quad (11)$$

The particle density, energy density and kinetic pressure are random variables in the grand-canonical ensemble. Their average values are

$$\begin{aligned} n &= \frac{1}{V} \sum_{\vec{p}} e^{(-E_{\vec{p}} + \mu)/T} \\ \epsilon &= \frac{1}{V} \sum_{\vec{p}} E_{\vec{p}} e^{(-E_{\vec{p}} + \mu)/T} \\ P &= \frac{1}{V} \sum_{\vec{p}} p_x v_x e^{(-E_{\vec{p}} + \mu)/T}, \end{aligned} \quad (12)$$

where p_x and v_x denote the components of the particle momentum and velocity along an arbitrary axis x . This expression of the kinetic pressure is obtained by evaluating the total momentum transferred per unit time by elastic collisions with a unit surface perpendicular to the x -axis. In other terms, it is the momentum flux along x . This definition will be used later. For a large volume, the sum over momenta is written as an integral:

$$\frac{1}{V} \sum_{\vec{p}} \rightarrow \int \frac{d^3 p}{(2\pi\hbar)^3}. \quad (13)$$

It is an instructive exercise to check that the kinetic pressure coincides with the thermodynamic pressure, i.e., that it satisfies the expected thermodynamic identities. The Gibbs–Duhem relation (6) gives $n = (\partial P / \partial \mu)_T$. On the other hand, the kinetic pressure (12) satisfies $(\partial P / \partial \mu)_T = P/T$. Putting together these two relations, we obtain

$$P = nT, \quad (14)$$

which is nothing but the ideal gas law. However, it is not obvious that P and n defined by (12) satisfy (14). This requires a little algebra. The velocity v_x is given by Hamilton's equation $v_x = \partial E_{\vec{p}} / \partial p_x$. One then writes

$$v_x e^{(-E_{\vec{p}} + \mu)/T} = -T \frac{\partial}{\partial p_x} (e^{(-E_{\vec{p}} + \mu)/T}). \quad (15)$$

Inserting this identity into (12), and integrating by parts over the variable p_x , one recovers (14).

In order to compute the pressure, one uses rotational symmetry of the integrand in (12), and one replaces $p_x v_x$ with $\vec{p} \cdot \vec{v}/3 = pv/3$. For massless particles, this gives immediately

$$P = \frac{\epsilon}{3}. \quad (16)$$

This relation holds approximately for a quark–gluon plasma at high temperatures, where interactions are small due to asymptotic freedom.

The integrals in (12) can easily be evaluated for massless particles. For a baryonless quark–gluon plasma ($\mu = 0$), this gives

$$n = \frac{g}{\pi^2 \hbar^3 C^3} T^3 \quad \epsilon = 3P = 3nT, \quad (17)$$

where g is the number of degrees of freedom (spin+colour+flavour), 16 for gluons and 24 for light u and d quarks, i.e., $g \approx 40$. Note that n denotes here the particle density, not the baryon density. (5) gives $\epsilon + P = Ts$, so that

$$s = 4n. \quad (18)$$

The entropy per particle is approximately 4 in a quark–gluon plasma (the ratio is in fact 3.6 for bosons, 4.2 for fermions).

For nonrelativistic particles, note that $P \ll \epsilon$. This is because ϵ includes the huge mass energy mc^2 .

3. Equations of relativistic hydrodynamics

Standard thermodynamics is about a system in global thermodynamic equilibrium. This means that intensive parameters (P , T , μ) are constant throughout the volume, and also that the system is globally at rest, which means that its total momentum is 0. In this section, we study systems whose pressure and temperature vary with space and time, and which are not at rest, such as the Indian atmosphere during monsoon. We, however, request that the system is in *local* thermodynamic equilibrium, which means that pressure and temperature are varying so slowly that for any point one can assume thermodynamic equilibrium in some neighbourhood about that point. Here, ‘neighbourhood’ has the same meaning as in mathematics, and there is no prescription as to the actual size of this neighbourhood or ‘fluid element’. There is, however, a general condition for local thermodynamic equilibrium to apply, which is that the mean free path of a particle between two collisions is much smaller than all the characteristic dimensions of the system. We come back to this important issue in section 6.

The fluid equations derived under the assumption of local thermodynamic equilibrium are called inviscid, or ideal-fluid, equations.

3.1. Fluid rest frame

The rest frame of a fluid element is the Galilean frame in which its momentum vanishes. All thermodynamic quantities associated with a fluid element (for example, ϵ , P , n) are defined in the rest frame. They are therefore Lorentz scalars by construction (for the same reason as the mass of a particle is a Lorentz scalar). Local thermodynamic equilibrium implies that the fluid element has isotropic properties in the fluid rest frame. This is a very strong assumption. It will be used extensively below. It is, in fact, the only non-trivial assumption of inviscid hydrodynamics.

3.2. Fluid velocity

The velocity \vec{v} of a fluid element is defined as the velocity of the rest frame of this fluid element with respect to the laboratory frame. The 4-velocity u^μ is defined by

$$u^0 = \frac{1}{\sqrt{1 - \vec{v}^2}} \quad \vec{u} = \frac{\vec{v}}{\sqrt{1 - \vec{v}^2}}, \quad (19)$$

where we have chosen a unit system where $c = 1$. u^0 is the Lorentz contraction factor. The 4-velocity transforms as a 4-vector under Lorentz transformations. The square of a 4-vector is a Lorentz scalar, and we indeed obtain

$$u^\mu u_\mu = (u^0)^2 - \vec{u}^2 = 1. \quad (20)$$

In hydrodynamics, the fluid velocity is a function of (t, x, y, z) , as are the thermodynamic quantities ϵ , P and n . The fluid velocity is also referred to as the ‘collective’ velocity.

3.3. Baryon number conservation

In nonrelativistic fluid dynamics, the equation of mass conservation is

$$\frac{\partial \rho}{\partial t} + \vec{\nabla} \cdot (\rho \vec{v}) = 0, \quad (21)$$

where ρ is the mass density. A relativistic conservation equation must take into account the Lorentz contraction of the volume by a factor u^0 . Recall that the baryon density n is always defined in the fluid rest frame. The baryon density in the moving frame is therefore nu^0 . Replacing ρ with nu^0 in the above equation and using $\vec{u} = u^0 \vec{v}$, one obtains the following covariant equation:

$$\partial_\mu (nu^\mu) = 0, \quad (22)$$

where we use the standard notation $\partial_\mu = \partial/\partial x^\mu$. This is a conservation equation for the 4-vector nu^μ . nu^0 is the baryon density and $n\vec{u}$ is the baryon flux.

In the rest frame of the fluid, the baryon flux vanishes. In nonrelativistic fluid dynamics, this is how the fluid rest frame is defined. In the relativistic case, the baryon flux could in principle be $\neq 0$ in the fluid rest frame, defined as the frame where the momentum density is zero: the momentum of baryons could be compensated by the momentum of baryonless particles (pions, gluons). However, local thermodynamic equilibrium implies isotropy. If there was a non-zero current, it would define a direction in space and isotropy would be lost. The baryon flux therefore vanishes in inviscid hydrodynamics. In relativistic viscous hydrodynamics, which studies deviations from local thermodynamic equilibrium, the baryon flux may be non-zero in the local rest frame: this transport phenomenon is called diffusion.

3.4. Energy and momentum conservation

The conservation of total energy and momentum gives four local conservation equations, each of which is analogous to the equation of baryon-number conservation. Baryon conservation gives a conserved current, which is a contravariant 4-vector $J^\mu = nu^\mu$. Energy and momentum are also a contravariant 4-vector, therefore the associated conserved currents can be written as a contravariant tensor $T^{\mu\nu}$, where each value of ν corresponds to a component of the 4-momentum, and each value of μ is a component of the associated current. Specifically,

- T^{00} is the energy density.
- T^{0j} is the density of the j th component of momentum, with $j = 1, 2, 3$.

- T^{i0} is the energy flux along axis i .
- T^{ij} is the flux along axis i of the j th component of momentum.

The momentum flux T^{ij} is usually called the pressure tensor. Kinetic pressure is precisely defined as the momentum flux (see section 2.4).

In the fluid rest frame, the assumption of local thermodynamic equilibrium strongly constrains the energy–momentum tensor. Isotropy implies that the energy flux T^{i0} and the momentum density T^{0j} vanish. In addition, it implies that the pressure tensor is proportional to the identity matrix, i.e., $T^{ij} = P\delta_{ij}$, where P is the thermodynamic pressure. The energy–momentum in the fluid rest frame is thus

$$T_{(0)} = \begin{pmatrix} \epsilon & 0 & 0 & 0 \\ 0 & P & 0 & 0 \\ 0 & 0 & P & 0 \\ 0 & 0 & 0 & P \end{pmatrix}. \quad (23)$$

In order to obtain the energy–momentum tensor in a moving frame, one does a Lorentz transformation. In what follows, we shall only need the expression of $T^{\mu\nu}$ to first order in the fluid velocity. To first order in the velocity \vec{v} , the matrix of a Lorentz transformation is

$$\Lambda = \begin{pmatrix} 1 & v_x & v_y & v_z \\ v_x & 1 & 0 & 0 \\ v_y & 0 & 1 & 0 \\ v_z & 0 & 0 & 1 \end{pmatrix}. \quad (24)$$

Under a Lorentz transformation, the contravariant tensor $T_{(0)}^{\mu\nu}$ transforms to

$$T^{\mu\nu} = \Lambda^\mu_\alpha \Lambda^\nu_\beta T_{(0)}^{\alpha\beta}, \quad (25)$$

which can be written as a multiplication of (4×4) matrices

$$T = \Lambda T_{(0)} \Lambda^T, \quad (26)$$

where Λ^T denotes the transpose of Λ . (24) shows that Λ is symmetric, $\Lambda^T = \Lambda$. Keeping only terms to order 1 in the velocity \vec{v} , (26) gives

$$T = \begin{pmatrix} \epsilon & (\epsilon + P)v_x & (\epsilon + P)v_y & (\epsilon + P)v_z \\ (\epsilon + P)v_x & P & 0 & 0 \\ (\epsilon + P)v_y & 0 & P & 0 \\ (\epsilon + P)v_z & 0 & 0 & P \end{pmatrix}. \quad (27)$$

We first note that $T^{\mu\nu}$ is symmetric: the momentum density T^{0i} and the energy flux T^{i0} are equal. This is because Lorentz transformations preserve the symmetries of tensors, and the tensor of the fluid at rest (23) is symmetric. The symmetry of $T^{\mu\nu}$ is a non-trivial consequence of relativity. In nonrelativistic fluid dynamics, the energy flux and the momentum density differ. (Recall that nonrelativistic energy does not include mass energy.) They have different dimensions: the ratio of energy flux to momentum density has the dimension of a velocity squared, which is dimensionless in relativity.

The momentum density is $(\epsilon + P)\vec{v}$. For a nonrelativistic fluid, it is $\rho\vec{v}$, where ρ is the mass density. Since $P \ll \epsilon$ and $\epsilon \simeq \rho\vec{v}$ in the nonrelativistic limit, we recover the correct limit. What replaces the mass density for a nonrelativistic fluid is not ϵ , as one would naïvely expect, but $\epsilon + P$: pressure contributes to the inertia of a relativistic fluid.

Finally, we prove that the energy–momentum tensor for an arbitrary fluid velocity is

$$T^{\mu\nu} = (\epsilon + P)u^\mu u^\nu - P g^{\mu\nu}, \quad (28)$$

where $g^{\mu\nu} \equiv \text{diag}(1, -1, -1, -1)$ is the Minkowski metric tensor. One easily checks that this equation reduces to (23) in the rest frame of the fluid, where $u^\mu = (1, 0, 0, 0)$. In addition, both sides of (28) are contravariant tensors, which means that they transform identically under Lorentz transformations. Since they are identical in one frame, they are identical in all frames, which proves the validity of (28).

The conservation equations of energy and momentum are

$$\partial_\mu T^{\mu\nu} = 0. \quad (29)$$

(22), (28) and (29) are the equations of inviscid relativistic hydrodynamics. Together with the equation of state of the fluid, which is defined as a functional relation between ϵ , P and n , they form a closed system of equations.

For the sake of simplicity, only continuous flows will be studied, in which all quantities vary continuously with spacetime coordinates. Inviscid hydrodynamics has a whole class of discontinuous solutions, which are called ‘shock waves’. The entropy of the fluid increases through a shock, while it is constant for a continuous flow (see section 4.3 and problem 1 in the appendix). Shock waves usually appear when the fluid undergoes compression, not expansion. They are therefore of limited relevance to heavy-ion collisions².

3.5. Sound waves

Sound is defined as a small disturbance propagating in a uniform fluid at rest. The energy density and pressure are written in the form

$$\epsilon(t, x, y, z) = \epsilon_0 + \delta\epsilon(t, x, y, z) \quad P(t, x, y, z) = P_0 + \delta P(t, x, y, z), \quad (30)$$

where ϵ_0 and P_0 correspond to the uniform fluid, and $\delta\epsilon$ and δP correspond to the small disturbance. To study the evolution of this disturbance, we linearize the equations of energy–momentum conservation by keeping only terms up to first order in $\delta\epsilon$, δP and \vec{v} . For this purpose, the expression (27) will suffice, since it is correct to first order in the velocity. (29) gives

$$\frac{\partial\epsilon}{\partial t} + \vec{\nabla} \cdot ((\epsilon + P)\vec{v}) = 0 \quad \frac{\partial}{\partial t}((\epsilon + P)\vec{v}) + \vec{\nabla} P = \vec{0}. \quad (31)$$

Inserting (30) and linearizing, these equations simplify

$$\frac{\partial(\delta\epsilon)}{\partial t} + (\epsilon_0 + P_0)\vec{\nabla} \cdot \vec{v} = 0 \quad (\epsilon_0 + P_0)\frac{\partial\vec{v}}{\partial t} + \vec{\nabla}\delta P = \vec{0}. \quad (32)$$

The first equation expresses that the density decreases if the velocity field diverges, $\vec{\nabla} \cdot \vec{v} > 0$, i.e., if the volume increases. This is energy conservation. The second equation is Newton’s second law, that the inertia of the fluid multiplied by its acceleration must be equal to the force. The force per unit volume is $-\vec{\nabla}\delta P$. It pushes the fluid towards lower pressure.

We now define the velocity of sound c_s by

$$c_s = \left(\frac{\partial P}{\partial \epsilon} \right)^{1/2}. \quad (33)$$

c_s^2 is inversely proportional to the compressibility of the fluid. A ‘soft’ equation of state corresponds to a small c_s . The derivative in (33) is well defined only if we specify along which line the partial derivative is taken. It will be shown in problem 1 that in ideal-fluid dynamics, the entropy per baryon of a fluid element is conserved as a function of time. If the

² In fact, shock waves do appear in the expansion when the equation of state has a first-order phase transition. These ‘rarefaction shocks’ produce little entropy, at most 7% [7].

fluid is initially uniform, then the entropy per baryon remains constant throughout the fluid at all times. This means that the partial derivative must be taken along the lines of constant entropy per baryon, s/n (thus corresponding to the adiabatic compressibility). In the case of a baryonless quark–gluon plasma, there is only one degree of freedom, and no ambiguity in defining the derivative. Using (6) and (7), one can rewrite c_s as

$$c_s = \left(\frac{d \ln T}{d \ln s} \right)^{1/2} \quad (34)$$

for a baryonless fluid.

Using the definition (33), we write $\delta P = c_s^2 \delta \epsilon$ in (32). We then eliminate \vec{v} between the two equations:

$$\frac{\partial^2(\delta \epsilon)}{\partial t^2} - c_s^2 \Delta(\delta \epsilon) = 0. \quad (35)$$

This is a wave equation in 3+1 dimensions, with velocity c_s . This equation means that small perturbations in a uniform fluid travel at the velocity c_s , independent of the shape of the perturbation: there is no sound dispersion in an inviscid fluid.

3.6. Ideal gas

If the interaction energies between the particles are small compared to their kinetic energies, one can express the hydrodynamic quantities in terms of the individual particle properties: conserved baryon number B , velocity \vec{v} and momentum p^μ . We use the notation v^μ for $(1, \vec{v})$ or, equivalently, $v^\mu = p^\mu/p^0$. Note that in spite of the notation, v^μ does not transform like a 4-vector under a Lorentz boost. The baryon current and energy–momentum tensor of a small fluid element of volume V are

$$nu^\mu = \frac{1}{V} \sum_{\text{particles}} B v^\mu \quad T^{\mu\nu} = \frac{1}{V} \sum_{\text{particles}} p^\nu v^\mu. \quad (36)$$

With these definitions, it is straightforward to check that nu^0 , T^{00} and T^{0i} correspond to the baryon, energy and momentum densities, respectively. The corresponding fluxes are obtained by weighting these quantities with the particle velocity \vec{v} .

Using the assumption of local thermodynamic equilibrium, one can replace these quantities with their thermal averages. The average number of particles with momentum \vec{p} is given by Boltzmann statistics (we neglect quantum statistics for simplicity) (11), where we replace $E_{\vec{p}}$ with the energy in the fluid rest frame E^* . Using (13), one can do the following substitution:

$$\frac{1}{V} \sum_{\text{particles}} \rightarrow \int \frac{d^3 p}{(2\pi\hbar)^3} e^{(-E^* + \mu)/T}. \quad (37)$$

This result will be useful later. We finally show that the expressions in (36) are covariant. For this purpose, we write $v^\mu = p^\mu/p^0$, and we note that $d^3 p/p^0$ is a Lorentz scalar, so that nu^μ and $T^{\mu\nu}$ are explicitly covariant.

4. Hydrodynamical expansion

The energy of a nucleus–nucleus collision at RHIC is 100 GeV per nucleon. This means that each incoming nucleus is contracted by a Lorentz factor $\gamma \approx 100$: nuclei are thin pancakes colliding. The collision creates thousands of particles in a small volume. These particles interact. If these interactions are strong enough, the system may reach a state of

local thermodynamic equilibrium. Equilibrium is at best local, certainly not global: global equilibrium applies to a gas in a closed box, which stays there for a long time and becomes homogeneous. The system formed in a heavy-ion collision starts expanding as soon as it is produced, and is far from homogeneous.

Can QCD tell whether or not the system reaches thermodynamic equilibrium? There is not yet an answer to this question, but a lot of progress has been made on this issue in recent years, due in particular to works on QCD plasma instabilities [8]. Another question is: can we tell from experimental data whether the system has reached local equilibrium? This issue will be briefly touched upon in section 6. You should keep in mind that local equilibrium is, at best, an approximation. Even if it turns out to give reasonable results, it is not the end of the story.

In this section, we assume that the system of interacting fields and particles produced in the collision reaches local thermodynamic equilibrium at some point. Its subsequent evolution follows the laws of inviscid hydrodynamics. Since there are first-order partial differential equations, their solution is uniquely determined once initial conditions are specified, together with an equation of state.

4.1. Initial conditions

The z -axis is chosen as the collision axis, and the origin is chosen such that the collision starts at $z = t = 0$. The two nuclei pass through each other in a time $t_{\text{coll}} \sim 0.15 \text{ fm}/c$ at RHIC. This time is a factor 100 smaller than the other characteristic dimension, the transverse size R of the nucleus. This clear hierarchy between the two scales is crucial.

The initial conditions are fixed at some initial time t_0 (or, more generally, on a spacelike hypersurface). A complete set of initial conditions involves the three components of fluid velocity, the energy density and the baryon density, at each point in space.

If the thermalization time t_0 is short enough, the transverse components v_x and v_y of the fluid velocity are zero. The reason is that the parton-parton collisions which produce particles occur on very short transverse scales. They produce particles whose transverse momenta are distributed isotropically in the transverse plane. Isotropy implies that there is no preferred direction and that the transverse momentum averaged over a fluid element vanishes. This part of the initial conditions is the only one on which there is fairly general agreement. This is the reason why the clearest experimental signatures of hydrodynamic behaviour are those associated with ‘transverse flow’, as we shall see below: if there is no transverse collective motion initially present in the system and if we see it in the data, it means that something has happened in-between which has to do with hydrodynamics.

We now discuss the initial value of the longitudinal flow velocity v_z . All particles are produced in a very short interval around $z = t = 0$. The standard prescription is that their longitudinal motion is uniform, so that their velocity is $v_z = z/t$: all particles at a given z have the same v_z , hence it is also the fluid velocity. This prescription is boost invariant, in the following sense: if one does a homogeneous³ Lorentz transformation with a velocity v along the z -axis, all three quantities v_z, z, t are transformed, but $v_z = z/t$ still holds in the new frame. This is because uniform motion remains uniform under a Lorentz transformation. This ‘boost-invariant’ prescription was first proposed by Bjorken [9], and it is supported by models inspired by high-energy QCD, such as the colour glass condensate.

We now introduce new coordinates, the proper time τ , the spacetime rapidity η_s and the fluid rapidity Y , defined by

³ A Lorentz transformation is homogeneous if it leaves the origin unchanged.

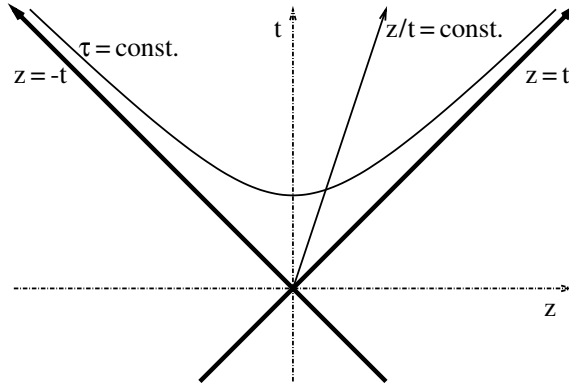


Figure 1. Nucleus–nucleus collision in the (z, t) plane. The thick lines are the trajectories of the colliding nuclei, which are moving nearly at the velocity of light. The lines of constant z/t are also lines of constant spacetime rapidity η_s .

$$t = \tau \cosh \eta_s \quad z = \tau \sinh \eta_s \quad v_z = \tanh Y. \quad (38)$$

Under a Lorentz boost in the z -direction, τ is unchanged, while η_s and Y are shifted by a constant. Lines of constant τ and constant η_s are represented in figure 1. Initial conditions are usually specified at a given proper time $\tau = \tau_0$, rather than at a given time $t = t_0$. Bjorken's prescription $v_z = z/t$ translates into $Y = \eta_s$: the fluid rapidity equals the spacetime rapidity.

We now discuss the initial density profile. One usually specifies the energy density, or the entropy density, as a function of x, y, η_s . There are constraints on these profiles, both theoretical and experimental, and prescriptions which satisfy these constraints. On the theoretical side, there is locality: it implies that a given point (x, y) in the transverse plane, the initial density can depend only on the thickness functions T_A and T_B of the two colliding nuclei at this point, defined as the integrals

$$T_{A,B}(x, y) = \int_{-\infty}^{+\infty} \rho_{A,B}(x, y, z) dz, \quad (39)$$

where $\rho_A(x, y, z)$ (resp. ρ_B) is the density of nucleons per unit volume in nucleus A (resp. B). The initial energy density is $\epsilon(x, y, \eta_s) = f(T_A(x, y), T_B(x, y), \eta_s)$, where f is some function. Various prescriptions can be found in the literature:

- The initial energy density is proportional to the density of binary collisions $T_A T_B$ [6].
- The initial entropy density is proportional to the density of participants [10], which is essentially $T_A + T_B$ on the overlap area and 0 outside. More complex prescriptions can also be found, where the entropy [11] or the energy [12] density is linear combinations of the densities of binary collisions and participants.
- In contrast to the above pictures, where the η_s dependence is fitted to measured rapidity spectra, the colour glass condensate [13] provides a prescription for the η_s dependence. It also predicts quite distinctive transverse profiles: at $z = \eta_s = 0$, it gives an initial multiplicity density approximately proportional to $\min(T_A, T_B)$ [14].

All these prescriptions reproduce well the observed centrality dependence of the global multiplicity.

We assume for simplicity a Gaussian entropy density profile at $\tau = \tau_0$:

$$s(x, y, \eta_s) \propto \exp\left(-\frac{x^2}{2\sigma_x^2} - \frac{y^2}{2\sigma_y^2} - \frac{\eta_s^2}{2\sigma_\eta^2}\right). \quad (40)$$

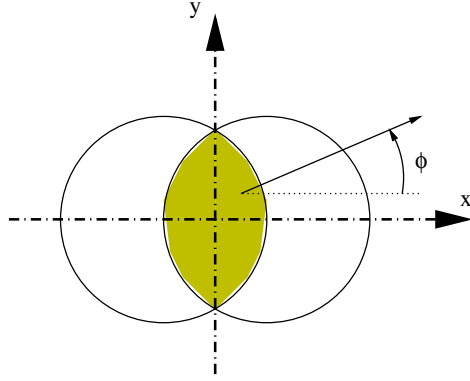


Figure 2. Non-central nucleus–nucleus collision in the transverse (x, y) plane. The x -axis is chosen as the direction of the impact parameter. The shaded area is the overlap area between the nuclei, where particles are produced. The density in this area can be approximated by a Gaussian, (40). The azimuthal angle of an outgoing particle with the x -axis is denoted by ϕ .

In this equation, σ_x and σ_y are the rms (root mean square) widths of the transverse distribution. For a central Au–Au collision, $\sigma_x = \sigma_y \simeq 3$ fm. For a non-central collision, one chooses in general the x -axis as the direction of impact parameter (see figure 2), and $\sigma_x < \sigma_y$. For a Au–Au collision at impact parameter $b = 7$ fm, $\sigma_x \simeq 2$ fm, $\sigma_y \simeq 2.6$ fm. Unlike σ_x and σ_y , σ_η is dimensionless. In order to estimate its value, we use the fact that the particle multiplicity is proportional to the entropy. We further assume, for the sake of simplicity, that the rapidity of outgoing particles is equal to their spacetime rapidity η_s . Rapidity distributions of outgoing particles in symmetric nucleus–nucleus collisions at RHIC are perfectly fit by Gaussians of width $\sigma_\eta \simeq 2.3$ [15].

4.2. Longitudinal acceleration

Our initial condition for the longitudinal fluid velocity is $v_z = z/t$ or, equivalently, $Y = \eta_s$. The original Bjorken picture [9] is that this relation holds at all times. We now discuss under which this condition is preserved by the hydrodynamical evolution. We first study the simple case $z = 0$. Since $v_z = 0$ initially at $z = 0$, we can use (31), which is valid to first order in the fluid velocity. The z component gives

$$\frac{\partial}{\partial t}((\epsilon + P)v_z) + \frac{\partial}{\partial z}P = 0. \quad (41)$$

Recalling that $v_z = 0$ initially, we obtain the acceleration:

$$\frac{\partial v_z}{\partial t} = -\frac{1}{\epsilon + P} \frac{\partial P}{\partial z} = -c_s^2 \frac{\partial \ln s}{\partial z}, \quad (42)$$

where we have used (10) and (33). If the initial density s depends on z , the fluid is accelerated, and the initial condition $v_z = 0$ is not preserved by the hydrodynamical evolution.

We now rewrite (42) using the variables η_s, τ, Y defined in (38). Near $z = 0$, $dt \simeq d\tau$, $dz \simeq \tau d\eta_s$, $v_z \simeq Y$:

$$\frac{\partial Y}{\partial \tau} = -\frac{c_s^2}{\tau} \frac{\partial \ln s}{\partial \eta_s}. \quad (43)$$

This equation can easily be generalized to $\eta_s \neq 0$ using boost invariance: any value of z with $|z| < t$ can be brought to $z = 0$ by means of a homogeneous Lorentz boost in the

z -direction. Such a boost leaves τ unchanged and shifts η_s by a constant. Hence it leaves $(\partial/\partial\eta_s)_\tau$ unchanged, and (43) holds for all η_s . The general condition under which $Y = \eta_s$ at all times is $(\partial s/\partial\eta_s)_\tau = 0$, corresponding to the limit $\sigma_\eta \rightarrow \infty$ in (40), i.e., to flat rapidity spectra.

We now show that even though rapidity spectra are not flat, the Bjorken picture is a reasonable approximation in practice at high energies. We follow the same approach as Eskola *et al* [16]. (40) and (43) give

$$\frac{\partial Y}{\partial \tau} = \frac{c_s^2 \eta_s}{\tau \sigma_\eta^2}. \quad (44)$$

Integrating from τ_0 to τ with the initial condition $Y = \eta_s$, we obtain our final result

$$Y(\tau) = \left(1 + \frac{c_s^2 \ln(\tau/\tau_0)}{\sigma_\eta^2} \right) \eta_s. \quad (45)$$

The rapidity of the fluid is not *equal* to the initial rapidity, as assumed in the Bjorken scenario, but *proportional* to it. As will be explained in section 4.6, transverse expansion acts as a cut-off for the longitudinal expansion at a time $\tau \sim 3.6$ fm/c for a central Au–Au collision. Even if the longitudinal pressure builds up as early as $\tau_0 \simeq 1$ fm/c, and assuming $c_s^2 = \frac{1}{3}$, this results in a modest increase of the rapidity width, by 9%. At LHC energies, where the rapidity width σ_η is expected to increase, effects of longitudinal acceleration will be even smaller.

4.3. Longitudinal cooling

We now derive the evolution of baryon density, energy density and entropy density in the Bjorken picture of a uniform longitudinal expansion. We assume that the transverse components of the velocity, together with their spatial derivatives, remain negligible. As will be shown in section 4.6, this is a good approximation as long as $t \ll \sigma_x/c_s, \sigma_y/c_s$.

We start with the baryon density. We rewrite (22) at $z = 0$. The Bjorken prescription $v_z = z/t$ gives $v_z = 0$ and $\partial v_z/\partial z = 1/t$:

$$\frac{\partial n}{\partial t} + \frac{n}{t} = 0. \quad (46)$$

This equation can be integrated as $nt = \text{constant}$, which expresses the conservation of the baryon number in a comoving fluid element: neglecting the transverse expansion, the volume of a comoving fluid element increases like the longitudinal size, i.e., like t .

The evolution of energy density at $z = 0$ is derived in a similar way, using (31):

$$\frac{\partial \epsilon}{\partial t} + \frac{\epsilon + P}{t} = 0. \quad (47)$$

The generalization of (46) and (47) for arbitrary z is obtained by transforming to (τ, η_s) coordinates, and replacing $(\partial/\partial t)_z$ with $(\partial/\partial \tau)_{\eta_s}$ and t with τ .

Unlike the baryon number, the total energy in a comoving fluid element is not conserved. (47) can be recast in the form

$$d(\epsilon t) = -P dt, \quad (48)$$

which shows that the comoving energy decreases. This is due to the negative work of pressure forces, $dE = -P dV$. This result is by no means trivial. It relies on our assumption of local equilibrium, which implies that the pressure is isotropic. P in (48) comes from T^{33} in (23), i.e., it is really the longitudinal pressure. For an ideal gas, (36) shows that $T^{33} = \sum_{\text{particles}} p_z v_z$. If the particles are initially produced with $v_z = z/t$ (as is for instance the case in the colour glass

condensate), the longitudinal pressure vanishes at $z = 0$. A non-zero longitudinal pressure can only appear as a result of the thermalization process. Most of the work on thermalization is about understanding how this longitudinal pressure appears.

It is worth noting that there is no direct evidence for longitudinal cooling (48) from experimental data. Experimental data are particles, which are emitted mostly at the final stage of the evolution. Our knowledge of initial stages is indirect. Longitudinal cooling implies a higher initial energy, for a given final energy. This can be observed only through a direct signature of the initial temperature. The most promising observables in this respect are electromagnetic observables, ‘thermal’ dileptons and photons, which are mostly emitted at the early stages, and sensitive to the temperature, but they are plagued by huge backgrounds. Although there is no experimental evidence for longitudinal cooling, it is clearly favoured theoretically: models of particle production based on perturbative QCD produce an initial energy significantly higher than the final energy, typically by a factor of 3 [17, 18], and require substantial longitudinal cooling to match with the data.

Finally, it is worth noting that the total entropy of a comoving fluid element is conserved, as the baryon number: (1) shows that $dE = -P dV$ and $dN = 0$ implies $dS = 0$. This is a general result for inviscid hydrodynamics (see problem 1 in the appendix). Physically, it means that there is no heat diffusion between fluid cells. To show this explicitly, we multiply (46) by μ and subtract (47). Using (5) and (7), one obtains

$$\frac{\partial s}{\partial t} + \frac{s}{t} = 0, \quad (49)$$

which shows that the comoving entropy, which scales like st , is constant.

4.4. Orders of magnitude

We can use experimental data to estimate the initial density in a heavy-ion collision. A popular estimate is Bjorken’s estimate of the energy density [9], defined as the ratio of the final ‘transverse’ energy (defined as $E \sin \theta$, where θ is the relative angle between the particle velocity and the collision axis, or polar angle) to the initial volume. This estimate neglects the longitudinal cooling (48), and therefore underestimates the initial energy density.

It is in fact probably safer to assume that the number of particles remains constant throughout the evolution: in the quark–gluon plasma phase, the particle number is approximately proportional to entropy (see (18)), and entropy is conserved. In the hadron phase, the scenario of chemical freeze-out (see below section 5.3) supports particle number conservation in the hadronic phase. Finally, at the quark–hadron phase transition, the idea of local quark–hadron duality (taken over from perturbative QCD [19, 20]) suggests that the number of particles might again be conserved. It is interesting to note that while perturbative QCD estimates fail in calculating the energy, they give a gluon multiplicity comparable to the observed multiplicity [17], which seems to support this assumption.

In order to estimate the initial density, we assume for simplicity that the longitudinal velocity of particles remains constant, i.e., $v_z = z/t$. Then, the particle density at time t is

$$n(t) = \frac{1}{S} \frac{dN}{dz} = \frac{1}{St} \frac{dN}{dv_z}, \quad (50)$$

where S is the transverse area of the interaction region, $S \approx \pi R^2 \approx 100 \text{ fm}^2$ for a central Au–Au collision, and N is the particle multiplicity. Since we are interested in the particle density in the fluid rest frame, we choose to estimate it near $z = 0$, where the fluid is at rest. The PHOBOS Collaboration has measured [21] the polar-angle distribution of charged

particles in central Au–Au collisions at 100 GeV per nucleon⁴. The result is $dN_{\text{ch}}/d\theta \simeq 700$ at $\theta = \pi/2$. Now, $v_z = v \cos \theta$. For particles emitted near $\theta = \pi/2$ with velocity v , this gives $dN/dv_z = (1/v) dN/d\theta$. The factor $(1/v)$ gives on average a factor 1.25, and charged particles are only 2/3 of the produced particles, so that $dN/dv_z \simeq 1300$. This gives numerically, for a central Au–Au collision at the top RHIC energy,

$$n(t) \simeq \frac{13}{t}, \quad (51)$$

where n is in fm^{-3} and t in fm/c .

This estimate must be compared with our estimate of the particle density in a quark–gluon plasma (17). Lattice QCD predicts that the transition to the quark–gluon plasma occurs near $T_c \approx 192 \text{ MeV}$ [22]. Since $\hbar c = 197 \text{ MeV fm}$, and we have chosen $c = 1$ throughout the calculations, (17) gives

$$n \simeq 3.75 \text{ fm}^{-3}, \quad (52)$$

at T_c . Comparing with (51), one sees that the system is above the critical density only if $t < 3.5 \text{ fm}/c$: the lifetime of the quark–gluon plasma is approximately $3.5 \text{ fm}/c$. This is of course a rough estimate: the density profile is not homogeneous throughout the surface S (the maximum density, at the centre, is approximately twice larger than the average density, and the lifetime is correspondingly larger), and we have neglected the transverse expansion (which, in contrast, reduces the lifetime). Finally, our starting assumption that the particle number is conserved is a crude picture for two reasons: the number of particles is ill-defined in a strongly-interacting system. Recent works have argued that the hadronization process could involve both fragmentation and recombination of partons, thus breaking the conservation of particle number at the transition [23].

4.5. The onset of transverse expansion

The initial transverse velocity of the fluid is 0, but the acceleration is in general not zero. It is given by an equation similar to (42):

$$\frac{\partial v_x}{\partial t} = -\frac{1}{\epsilon + P} \frac{\partial P}{\partial x} = -c_s^2 \frac{\partial \ln s}{\partial x}, \quad (53)$$

and a similar equation along the y -axis. Inserting (40) into (53), and assuming constant c_s for simplicity, we integrate over t to obtain, for small t ,

$$v_x = \frac{c_s^2 x}{\sigma_x^2} t, \quad v_y = \frac{c_s^2 y}{\sigma_y^2} t. \quad (54)$$

Note that we have integrated from $t = 0$. Thermalization certainly requires some time, and hydrodynamics cannot apply at very early times. On the other hand, the system is expanding freely in the vacuum, and it is clear that the transverse expansion starts immediately: it does not wait until thermalization is achieved, so that it is probably reasonable to start the transverse expansion at $t = 0$.

(54) shows that the transverse expansion, unlike the longitudinal expansion, is a very smooth process. This may not be intuitive: the pressure is very high at early times, and pressure gradients are largest too, so that a huge force $-\vec{\nabla}P$ acts on the system; but this is compensated by the large inertia $\epsilon + P$, resulting in a linear increase of the transverse fluid velocity. The typical time scale for transverse expansion is σ_x/c_s , which means that longitudinal expansion dominates for $t \ll \sigma_x/c_s$.

⁴ What is measured is in fact the pseudorapidity (η) distribution, defined by $dN/d\eta = \sin \theta dN/d\theta$, which coincides with the polar-angle distribution near $\theta = \pi/2$.

The almond shape of the overlap area, in a non-central collision (see figure 2), results in $\sigma_x < \sigma_y$, which in turn implies $\langle v_x^2 \rangle > \langle v_y^2 \rangle$, where the angular brackets denote averages weighted with the initial density: the transverse expansion is larger along the smaller dimension, because the pressure gradient is larger. This results in more particles emitted near $\phi = 0$ and $\phi = \pi$, i.e., parallel to the x -axis, than near $\phi = \pm\pi/2$, parallel to the y -axis [24]. This effect corresponds to a $\cos 2\phi$ term in the Fourier decomposition of the azimuthal distribution:

$$\frac{dN}{d\phi} \propto 1 + 2v_2 \cos 2\phi, \quad (55)$$

where v_2 is a positive coefficient, which is called ‘elliptic flow’. The observed dependence of v_2 on transverse momentum and particle species is considered the most solid evidence for hydrodynamical behaviour in nucleus–nucleus collision. It will be studied in section 5.4.

4.6. The time scale of transverse expansion

Our equation for longitudinal cooling (48) was derived by neglecting transverse expansion. If there was no transverse expansion, the system would cool forever and no energy would be left in the central rapidity region. Transverse expansion effectively acts as a cut-off for longitudinal cooling. The typical time when transverse expansion becomes significant is, for dimensional reasons, σ_x/c_s or σ_y/c_s . A convenient scaling variable is provided by the following quantity [25]:

$$R \equiv \left(\frac{1}{\sigma_x^2} + \frac{1}{\sigma_y^2} \right)^{-1/2}. \quad (56)$$

The total transverse energy can be computed, to a very good approximation, by assuming that (48) holds until $t = R/c_s$, and that the energy remains constant for $t > R/c_s$ [10]. This is what I mean by saying that transverse expansion acts as a cut-off for longitudinal cooling.

An important feature of hydrodynamical models is that the momentum distributions of outgoing particles depend on the equation of state, therefore experimental data constrain the equation of state. Most of this dependence is a consequence of the simple picture above: after $t = R/c_s$, the energy and entropy of the fluid are essentially constant. Since the multiplicity is proportional to the entropy, this also implies that the average energy per particle remains constant. The transverse energy per particle thus reflects the thermodynamic state of the system at $t \approx R/c_s$. Since the energy per particle scales like the temperature (see (17)), it gives a direct information on the temperature of the system at $t \approx R/c_s$. The entropy density at this time is proportional to the particle density, derived in section 4.4. Experimental data imply a low temperature, which in turn means that the equation of state is ‘soft’ (see (34)). Hydrodynamical models favour a soft equation of state, even softer than predicted by lattice QCD.

Quite naturally, R/c_s is also the characteristic time for the build-up of elliptic flow: v_2 at $t = R/c_s$ is typically half its final value. With $c_s = 1/\sqrt{3}$, the numerical value of R/c_s for a Au–Au collision is 3.6 fm/c for $b = 0$ (central collision), 2.7 fm/c for $b = 7$ fm. This explains why elliptic flow is considered a signature of early pressure.

The final value of elliptic flow is a good illustration of how the choice of initial conditions may influence the results. Early hydrodynamical calculations had predicted a v_2 as large as seen at RHIC, and this was the main reason for the success of inviscid hydrodynamics. However, the possibility was raised recently that this agreement might be due to unrealistic

initial conditions. Let us briefly explain why. Hydrodynamics predicts that v_2 is proportional to the eccentricity ε of the initial distribution, defined as

$$\varepsilon \equiv \frac{\sigma_y^2 - \sigma_x^2}{\sigma_y^2 + \sigma_x^2}. \quad (57)$$

Early hydrodynamical calculations estimated ε using participant scaling or binary collision scaling (see section 4.1). It was discovered recently that the colour glass condensate predicts a significantly higher eccentricity [11, 26].

Another effect may increase the initial eccentricity and was suggested by experimental data: one expects ε to vanish for central collisions but, experimentally, a non-zero v_2 is seen even for the most central collisions. Surprisingly, the effect is larger with smaller nuclei: the value of v_2 in central Cu–Cu collisions is almost twice as large as in central Au–Au collisions. The PHOBOS Collaboration has suggested that this may be due to fluctuations in the positions of nucleons within the nuclei [27–29]. There have been several attempts by STAR and PHOBOS to measure these fluctuations directly, but they are difficult to isolate from other effects. The present situation is that our knowledge of the initial density profile is much more uncertain than was usually thought a few years ago.

5. Particle spectra and anisotropies

The fluid eventually becomes free particles which reach the detector. In this section, we derive some properties of the momentum distribution of particles emitted by a fluid. The transition between a fluid (where the particles undergo many collisions) and free particles cannot be described by fluid mechanics itself. If inviscid hydrodynamics holds throughout most of the expansion, one can reasonably assume that the late stages of the expansion do not alter the essential features of the momentum distributions. We therefore assume that the momentum distribution of outgoing particles is essentially the momentum distribution of particles within the fluid, towards the end of the hydrodynamical expansion, and that the fluid consists of independent particles (ideal gas). These assumptions form the basis of the common ‘Cooper–Frye freeze-out picture’ [30]. Here, we further assume that the fluid is baryonless and that momentum distributions are given by Boltzmann statistics:

$$\frac{dN}{d^3x d^3p} = \frac{2S + 1}{(2\pi\hbar)^3} \exp\left(-\frac{E^*}{T}\right), \quad (58)$$

where $2S + 1$ is the number of spin degrees of freedom and E^* is the energy of the particle in the fluid rest frame. T is called the freeze-out temperature.

5.1. Comoving particles and fast particles

The Boltzmann factor (58) is maximum when the energy E^* in the fluid rest frame is minimum. For a given fluid velocity, E^* is minimum when the particle is at rest in the fluid rest frame, in which case $E^* = m$. This in turn means that the particle velocity in the laboratory equals the fluid velocity: the particle is comoving with the fluid and has a momentum $p^\mu = mu^\mu$. For light particles, this corresponds to low transverse momenta: even if the fluid has a transverse velocity as large as 0.7, the corresponding transverse momentum is approximately equal to the mass, i.e., only 140 MeV/c for pions, 500 MeV/c for kaons. In this low-momentum region, the momentum distribution depends on how the fluid velocity is distributed, and few general results can be obtained.

In this section, we study particles which move faster than the fluid, which we call ‘fast particles’. For fast particles, E^* is larger than m . For a given momentum \vec{p} of the particle,

the minimum of E^* occurs if the fluid velocity is parallel to \vec{p} : fast particles are more likely to be emitted from regions where the fluid velocity is parallel to their velocity (which means that the fluid and the particle have the same azimuthal angle ϕ and rapidity y). This result can be justified rigorously using the saddle-point method [31]. For simplicity, we study particles emitted at $\theta = \pi/2$, i.e., $p_z = 0$ (zero rapidity), and we derive properties of the transverse momentum distributions. Since the transverse momentum is invariant under Lorentz boosts along z , our final results are also valid at non-zero rapidity.

The energy of the particle in the fluid rest frame can be generally written as $E^* = p^\mu u_\mu$ in the laboratory frame. The reason is twofold: (1) $p^\mu u_\mu$ is a Lorentz scalar and is independent of the frame where it is evaluated; (2) $p^\mu u_\mu$ reduces to p^0 if the fluid velocity is zero. Assuming that the fluid velocity is parallel to the particle velocity, and that $p_z = 0$, we obtain

$$E^* = p^\mu u_\mu = m_t u^0 - p_t u, \quad (59)$$

where $u^0 = \sqrt{1+u^2}$, p_t is the transverse momentum of the particle and $m_t = \sqrt{p_t^2 + m^2}$ its ‘transverse mass’, which equals the energy for a particle with $p_z = 0$. The definition of a fast particle is that its velocity exceeds the maximum fluid velocity, i.e., $p_t > mu$ (or, equivalently, $m_t > mu^0$) everywhere. For a fast particle, E^* is minimum if u is maximum: fast particles are emitted from the regions where the fluid velocity is largest.

5.2. Radial flow

We first study the transverse momentum distribution of particles emitted in central collisions. Rotational symmetry in the transverse plane allows us to write $dp_x dp_y = 2\pi p_t dp_t$. (58) and (59) then give

$$\frac{dN}{2\pi p_t dp_t dp_z} \propto \exp\left(\frac{-m_t u^0 + p_t u}{T}\right), \quad (60)$$

where u is the maximum transverse fluid 4-velocity at zero rapidity, according to the above discussion. If the fluid is at rest, i.e., $u = 0$ and $u^0 = 1$, one expects that the spectra are exponential in m_t , with the same slope $1/T$ for all particles. It is a general feature of Boltzmann statistics that kinetic energies associated with thermal motion are always of order T and independent of the particle mass. This is precisely what is seen in proton–proton collisions: figure 3 displays the momentum distributions of various hadrons in log scale, as a function of the transverse mass. N denotes the number of particles per event. Pions, kaons, protons and antiprotons are on parallel lines. Protons are slightly above antiprotons: this shows that the net baryon number is not strictly zero and that our ‘baryonless’ picture is only an approximation. The lines of protons and antiprotons are above the line of pions (if one extrapolates the latter to larger m_t), roughly by a factor 2. This factor 2 corresponds to the spin degrees of freedom in (58): $S = \frac{1}{2}$ for protons and 0 for pions and kaons. By contrast, the kaon line is lower than the pion line. This phenomenon is known as ‘strangeness suppression’: less strange particles are produced in elementary particles than expected on the basis of statistical models.

The fact that thermal models give a satisfactory description of particle spectra and abundances in p–p [33], and even e^+e^- collisions [34] does not prove that thermal equilibrium, is achieved in these collisions. In fact, thermal equilibrium is not at all expected in such small systems, and the apparent thermal behaviour still remains a puzzle. It could arise from the mechanism of hadronization itself, which is essentially a statistical process.

We now show that m_t -scaling is broken if the fluid moves: on top of thermal motion, there is now a collective velocity v , the fluid velocity, which applies to all particles within the fluid. The kinetic energy associated with this collective motion is $mv^2/2$ in the nonrelativistic limit. It increases with the particle mass, and one expects that heavier particles will have larger

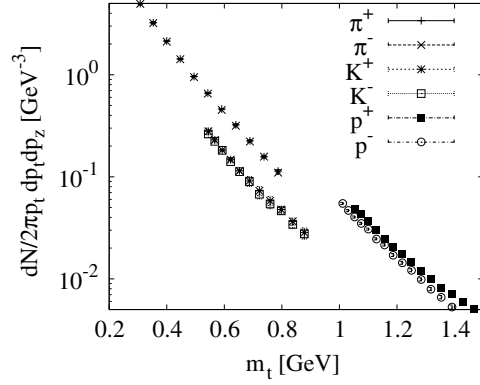


Figure 3. m_t spectra of identified hadrons produced in p–p collisions near $p_z = 0$ (data from [32], replotted).

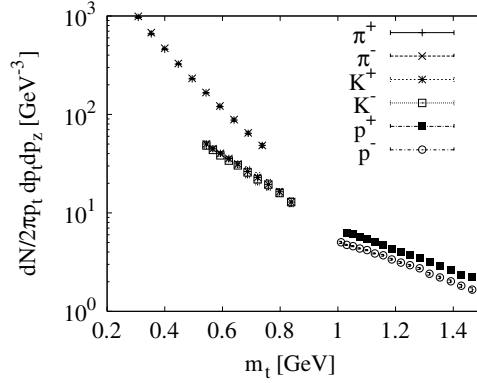


Figure 4. m_t spectra of identified hadrons produced in central Au–Au collisions near $p_z = 0$ (data from [32], replotted). Yields are normalized per event, which explains why they are $\approx 200\times$ larger than in p–p collisions.

kinetic energies if collective flow is present. To see the breaking of m_t -scaling explicitly, we compute the slope of the m_t spectrum by taking the log of (60) and differentiating with respect to m_t . We use the fact that $p_t^2 = m_t^2 - m^2$ implies $dp_t/dm_t = m_t/p_t$:

$$\frac{d}{dm_t} \log \left(\frac{dN}{2\pi p_t dp_t dp_z} \right) = \frac{-u_0 + um_t/p_t}{T}. \quad (61)$$

For a given m_t , heavier particles have a smaller p_t . If $u > 0$, this gives a positive contribution to the slope, resulting in flatter m_t -spectra⁵. This is clearly seen in Au–Au collisions (figure 4): (anti)proton spectra and kaon spectra are much flatter than pion spectra. This is generally considered evidence for transverse flow [35]. In the case of central collisions, which have rotational symmetry in the (x, y) plane, transverse flow is also called ‘radial’ flow.

⁵ Note that (61) applies only to fast particles, for which $p_t > mu$ and $m_t > mu_0$, so that the slope is always negative.

5.3. Chemical versus kinetic freeze-out

Comparing figures 3 and 4, it is clear that the relative abundances of pions, kaons, and (anti)protons, also known as particle ratios, do not change dramatically from proton–proton to Au–Au collisions: what happens between proton–proton and Au–Au is essentially a redistribution of the transverse masses for heavier particles.

Now, the number of particles of a given type emitted by a fluid element is obtained by integrating the Boltzmann factor (58) over momentum. As a consequence, particle ratios only depend on the temperature. The fact that particle ratios are the same in proton–proton and Au–Au collisions means that the temperature is the same: the temperature extracted from particle ratios is called the ‘chemical freeze-out temperature’, and its value is $T_c \simeq 170$ MeV [36]. A detailed calculation shows that the kaon/pion ratio is in fact larger in Au–Au collisions than in proton–proton collisions and that there is no ‘strangeness suppression’ in Au–Au collisions. Although this is generally considered a strong argument for thermalization, it has been shown that the mechanism of quark production itself can produce apparent thermal equilibrium [37].

While the same value of the temperature explains both the particle ratios and the m_t spectra in proton–proton collisions, it is no longer the case for Au–Au collisions. If T in (61) was the same for proton–proton and Au–Au collisions, transverse flow would result in much flatter pion spectra for Au–Au than proton–proton collisions. The phenomenon of transverse (or radial) flow nicely explains the slopes of m_t spectra of identified hadrons, but the price to pay is a lower value of the temperature. This temperature is referred to as the temperature of ‘kinetic freeze-out’, and its typical value at RHIC is $T_f \simeq 100$ MeV.

The fact that $T_f < T_c$ is usually interpreted in the following way: inelastic collisions, which maintain chemical equilibrium, stop below T_c ; below T_c , particle abundances are frozen, but there are still enough elastic collisions to maintain Boltzmann distributions of momenta, i.e., kinetic equilibrium. Kinetic equilibrium is eventually broken when the temperature becomes lower than T_f , the kinetic freeze-out temperature.

5.4. Elliptic flow

We now study non-central collisions, and we define the x - and y -axes as in figure 2. We rewrite (58) using $dp_x dp_y = p_t dp_t d\phi$ and (59), where we take into account the fact that the maximum fluid velocity at zero rapidity may also depend on ϕ :

$$\frac{dN}{p_t dp_t dp_z d\phi} \propto \exp\left(\frac{-m_t u_0(\phi) + p_t u(\phi)}{T}\right). \quad (62)$$

According to (54), the fluid velocity is larger on the x -axis than on the y -axis, which is the phenomenon referred to as elliptic flow. This effect can be parameterized in the form

$$u(\phi) = u + 2\alpha \cos 2\phi, \quad (63)$$

where α is a positive coefficient characterizing the magnitude of elliptic flow and u is the average over ϕ of the maximum fluid 4-velocity in the ϕ -direction. In semi-central Au–Au collisions at RHIC, experimental data suggest that $\alpha \simeq 4\%$, which means that elliptic flow at the level of the fluid is a small effect. Using $u^0 = \sqrt{u^2 + 1}$, and expanding to first order in α , we obtain

$$u^0(\phi) = u^0 + 2v\alpha \cos 2\phi, \quad (64)$$

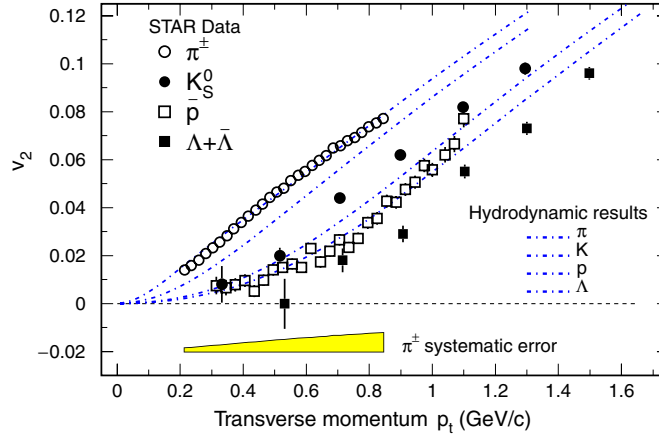


Figure 5. Elliptic flow of identified hadrons as a function of transverse momentum [39]. v_2 versus p_t is often called ‘differential’ elliptic flow.

where $v \equiv u/u_0$ is the average over ϕ of the maximum fluid velocity. We then insert (63) and (64) into (62) and expand to first order in α . Comparing with (55), we obtain the value of elliptic flow, v_2 :

$$v_2 = \frac{\alpha}{T} (p_t - v m_t). \quad (65)$$

This equation [38] explains the essential features of the differential elliptic flow of identified particles, as shown in figure 5. For light particles such as pions, $m_t \simeq p_t$, and v_2 increases essentially linearly with p_t . This is already a non-trivial result. For heavier particles, m_t is larger at the same value of p_t , resulting in smaller v_2 .⁶ This strong mass ordering is clearly seen in the data: kaons and protons have smaller v_2 than pions at the same p_t . (65) shows that the mass ordering is significant only if v is a significant fraction of the velocity of light. RHIC data on v_2 can therefore be considered strong evidence for *relativistic* collective flow. Fits to data suggest that the maximum fluid velocity may be as large as 0.7.

The increase of v_2 with p_t predicted by (65) is seen in the data only up to $p_t \sim 2$ GeV/ c . For higher values of p_t , v_2 saturates and eventually decreases [40]. Such a deviation from ideal hydrodynamics has been shown to occur generally as a result of viscous effects [41], to be discussed briefly in section 6. However, viscosity alone cannot explain the observation [42] that v_2 becomes *higher* for baryons than for mesons between 2 and 3 GeV/ c , an effect which has been attributed to the process of hadronization through quark coalescence [43]. This picture has in turn suggested new analyses involving new scaling variables [44]. This illustrates the vivid interplay between experiment and phenomenology in the field of heavy-ion collisions.

6. Viscosity and thermalization

6.1. Types of flows

The various types of flows occurring in fluid mechanics are classified according to the values of three dimensionless parameters:

⁶ Note that (65) only applies to fast particles, $p_t > mu$ and $m_t > mu_0$, which implies $v_2 > 0$.

- The Knudsen number $Kn \equiv \lambda/R$ is the ratio of the mean free path λ of a particle between two collisions, to a characteristic spatial dimension of the system, R . Applicability of hydrodynamics requires $Kn \ll 1$.
- The Mach number $Ma \equiv v/c_s$ is the ratio of the characteristic flow velocity, v , to the sound velocity, c_s . It can be shown (see problem 2 in the appendix) that if $Ma \ll 1$, the density is almost uniform throughout the fluid, which defines *incompressible* flow: whether a fluid is compressible or not depends on how fast it is flowing.
- The Reynolds number is defined by $Re \equiv Rv/(\eta/\rho)$, where η is the shear viscosity and ρ the mass density (which must be replaced with $\epsilon + P$ for a relativistic fluid), and R and v are defined as above. If $Re \gg 1$, the flow can be considered inviscid.

There is a fundamental relation between these three numbers. Transport theory indeed shows that $\eta/\rho \sim \lambda c_s$, which implies

$$Re \times Kn \sim Ma. \quad (66)$$

This is a very general relation⁷. Since the validity of a fluid description requires $Kn \ll 1$, (66) shows that there are essentially three types of flows, which correspond to three different branches of fluid dynamics.

- Compressible flows, for which Ma is of order unity. Since $Kn \ll 1$, this in turn implies $Re \gg 1$: compressible flows are inviscid. This part of fluid mechanics is called gas dynamics.
- Viscous flows, for which Re is of order unity. Since $Kn \ll 1$, this in turn implies $Ma \ll 1$: viscous flows are incompressible.
- Incompressible, inviscid flows (sometimes called ‘ideal’), for which $Ma \ll 1$ and $Re \gg 1$. This is where turbulence occurs.

In the case of a heavy-ion collision, the fluid is expanding into the vacuum: this is obviously a compressible flow, where Ma is of order unity. The real question is the validity of the fluid description, i.e., the actual value of Kn .

6.2. Viscous corrections

The dynamics of gases expanding into the vacuum has been extensively studied in nonrelativistic gas dynamics [45]. The Knudsen number Kn provides a natural small parameter for these problems, and observables can be computed by an expansion in powers of Kn :

- The lowest order, i.e., the limit $Kn \rightarrow 0$, corresponds to inviscid hydrodynamics.
- The first correction, linear in Kn , is also linear in the viscosity, since $Kn \propto 1/Re \propto \eta$. The corresponding fluid equations are Navier–Stokes equations or viscous hydrodynamics. They involve several transport coefficients (diffusion, shear and bulk viscosities), and the energy–momentum tensor is no longer symmetric.
- The next correction, in Kn^2 , is described by more complicated equations called the Burnett equations [46, 47].

A heavy-ion collision at RHIC produces a few thousand particles. It is intuitively obvious that the fluid picture is at best an approximation and that there are sizeable corrections to this picture. The question of whether or not hydrodynamics applies to heavy-ion collisions is no longer a qualitative question, but rather a quantitative one. This is what viscosity is about:

⁷ There is a dimensionless proportionality constant of order 1 between the two sides of (66), whose precise values depends on the interaction. It is $\simeq 1.6$ for a dilute gas of nonrelativistic hard spheres.

the goal of viscous hydrodynamics is to provide a more accurate description of heavy-ion collision, by taking into account the leading corrections to the ideal-fluid picture [48, 49].

We conclude with estimates of the Knudsen number at RHIC. The actual value of the viscosity of hot QCD is not known at present. Estimates have been obtained from lattice QCD [50] but there are still controversies. Interestingly, a universal lower bound on the viscosity to entropy ratio, which might hold for all field theories, has been proposed on the basis of a correspondence with black-hole physics [51]. This universal bound is

$$\frac{\eta}{s} > \frac{\hbar}{4\pi}. \quad (67)$$

This lower bound on η can be converted into an upper bound on the Reynolds number. Since $Kn \sim 1/Re$, this in turn gives a lower bound on the Knudsen number, which is of order 0.1 for central Au–Au collisions. This means that viscous corrections at RHIC are expected to be 10% at least. A recent study of elliptic flow [52] suggests that the magnitude of viscous corrections is at least 30%. This in turn would mean that the viscosity of hot QCD is significantly larger than the KSS bound (67).

Inviscid hydrodynamics gives a satisfactory explanation of several RHIC data at the qualitative level: mass ordering of m_t spectra, differential elliptic flow. However, they are unable to reproduce all the data quantitatively. Taking into account viscous corrections will be a major step in this respect. This is an ongoing programme. A lot of progress has already been made, and quantitative results, with comparison to RHIC data, are now appearing [53]. Eventually, one should be able to estimate both the equation of state and the viscosity of hot QCD from heavy-ion experiments. Hydrodynamic calculations may even shed light on the initial density profile, i.e., on the early stages of the collision, and the particle production itself. Hydrodynamics was crucial in our understanding of heavy-ion collisions at RHIC. It will be even more important at LHC, where the quark–gluon plasma will last longer than at RHIC, and the whole expansion will be dominated by hydrodynamics.

Acknowledgments

I thank IIT Mumbai and TIFR for their hospitality, CEFIPRA for financial support under project 3104-3, and F Grassi and R Bhalerao for discussions and useful comments on the manuscript.

Appendix A. Problems

Problem 1. Equations of inviscid hydrodynamics

- (1) We introduce the notations $D \equiv u^\mu \partial_\mu$ and $\Delta^{\mu\nu} \equiv g^{\mu\nu} - u^\mu u^\nu$. How do these quantities simplify for a fluid at rest?
- (2) Using (20), show that $u_\nu \partial_\mu u^\nu = 0$ and $\Delta_{\mu\nu} u^\nu = 0$.
- (3) Multiply the equations of energy–momentum conservation (28) and (29) by u_ν and show that $u^\mu \partial_\mu \epsilon + (\epsilon + P) \partial_\mu u^\mu = 0$.
- (4) Using (5), (7) and (22), show that $\partial_\mu (s u^\mu) = 0$. What is the interpretation of this equation?
- (5) Show that $D(s/n) = 0$. What is the interpretation of this result?
- (6) Multiply the equations of energy–momentum conservation by $\Delta_{\rho\nu}$ and show that

$$(\epsilon + P) D u_\rho = \Delta_{\rho\nu} \partial^\nu P. \quad (A.1)$$

What is the nonrelativistic limit of this equation?

- (7) Explain why the previous equation, together with the equation of entropy conservation and baryon-number conservation, exhausts all the information contained in the equations of hydrodynamics.

Problem 2. Steady flows

The flow in a heavy-ion collision is strongly time dependent. Studying steady flows is somewhat academic in this context. However, simple exact results can be easily obtained for steady flows, and they provide useful insight into the physics of hydrodynamics.

- (1) Show that (A.1) for $\rho = 0$, in the case of a steady flow (where all quantities are time independent), can be recast in the form

$$d \ln u^0 = - \frac{dP}{\epsilon + P}, \quad (\text{A.2})$$

where the differential is taken along a streamline (i.e., a line parallel to the fluid velocity).

- (2) Take the nonrelativistic limit of this result for an incompressible fluid and comment on the result.
 (3) For a baryonless fluid, show that $u^0 T$ is constant along a streamline.
 (4) The velocity of sound c_s is defined as $c_s = \sqrt{dP/d\epsilon}$. Show that the result of Q1 can be rewritten as

$$\frac{du}{u} = - \frac{c_s^2}{v^2} \frac{ds}{s}, \quad (\text{A.3})$$

where $v = u/u^0$ is the fluid velocity. The Mach number of a flow is defined by $\text{Ma} \equiv v/c_s$. If $\text{Ma} \ll 1$, one says that the flow is incompressible. Explain why?

- (5) Consider an elementary flux tube, and denote by Σ the cross-section area of the flux tube at some point. Explain why $su\Sigma$ is a constant along the flux tube. Write this in differential form.
 (6) Eliminate the fluid 4-velocity u between the results of Q4 and Q5 and show that

$$\frac{d\Sigma}{\Sigma} = \left(\frac{c_s^2}{v^2} - 1 \right) \frac{ds}{s} \quad (\text{A.4})$$

along the flux tube. How does the density evolve diverging streamlines, depending on whether the flow is supersonic or subsonic?

- (7) Consider the case where a nozzle emits a baryonless gas, which then expands into the vacuum. List some consequences of the results obtained in this problem.

Problem 3. The Riemann problem

The Riemann problem is a one-dimensional time-dependent flow which can be solved exactly. The initial conditions are: at time $t = 0$, the half space $x < 0$ is filled with a uniform fluid at rest, with energy density ϵ_0 , while the half space $x > 0$ is empty. We shall determine the flow profile at $t > 0$. Since there is no characteristic length or time scale in the problem, both the fluid velocity and the density depend through x and t only through the combination $\zeta = x/t$: the flow profile has the same shape at all positive times, only its size increases linearly with time.

- (1) Sketch the density profile at positive time.
 (2) We first determine the point where the matter starts to flow to the right. At this point the fluid velocity is 0 by continuity, but the derivatives of v with respect to x and t are

generally not 0. (31) simplify to

$$\frac{\partial \epsilon}{\partial t} + (\epsilon + P) \frac{\partial v}{\partial x} = 0 \quad \frac{\partial P}{\partial x} + (\epsilon + P) \frac{\partial v}{\partial t} = 0. \quad (\text{A.5})$$

Rewrite these partial differential equations as ordinary differential equations in the reduced variable $\zeta = x/t$.

- (3) Eliminate the pressure from this equation using $dP = c_s^2 d\epsilon$. Show that the resulting system of equations has a non-trivial solution only if $\zeta = \pm c_s$. In the situation considered here, one expects $d\epsilon/d\zeta < 0$ and $dv/d\zeta > 0$. Show that this implies $\zeta = -c_s$. At which value of ζ does the matter start to flow? Comment on this result.
- (4) Since the equations are Lorentz invariant, at every point one can perform a Lorentz boost such that the fluid velocity is 0 in the new frame. Explain, without algebra, why the above result generalizes to $\zeta = (v - c_s)/(1 - vc_s)$ at a point where the fluid velocity is not zero?
- (5) Invert this relation and draw the velocity profile as a function of x for an ideal quark–gluon plasma with sound velocity $c_s = 1/\sqrt{3}$.

Appendix B. Solutions

B.1. Solution of problem 1

- (1) $D = u^0(\partial_t + \vec{v} \cdot \vec{\nabla})$ where $\vec{v} = \vec{u}/u^0$ is the fluid velocity. In the nonrelativistic limit, $u^0 = 1$ and D is the convective derivative, i.e., the time derivative along a comoving fluid element. For a fluid at rest, D is the time derivative and $\Delta^{\mu\nu} = \text{diag}(0, -1, -1, -1)$ projects spacetime onto space.
- (2) By taking the derivative of $u^\nu u_\nu = 1$, one obtains $u_\nu \partial_\mu u^\nu = 0$. From the definition of $\Delta_{\mu\nu}$ it is obvious that $\Delta_{\mu\nu} u^\nu = 0$.
- (3) The equation of energy–momentum conservation can be written as the sum of three terms:

$$(\epsilon + P)u^\mu \partial_\mu u^\nu + \partial_\mu((\epsilon + P)u^\mu)u^\nu - \partial^\nu P = 0. \quad (\text{B.1})$$

Multiplying this equation by u_ν , the first term disappears using the result of Q2. One obtains

$$\partial_\mu((\epsilon + P)u^\mu) - u^\mu \partial_\mu P = 0. \quad (\text{B.2})$$

Expanding the first term, one obtains

$$u^\mu \partial_\mu \epsilon + (\epsilon + P) \partial_\mu u^\mu = 0. \quad (\text{B.3})$$

- (4) (22) gives

$$u^\mu \partial_\mu n + n \partial_\mu u^\mu = 0. \quad (\text{B.4})$$

Multiplying by μ and subtracting from the previous equation, one obtains

$$u^\mu T \partial_\mu s + Ts \partial_\mu u^\mu = 0. \quad (\text{B.5})$$

Simplifying by T , this can be recast in the form $\partial_\mu(su^\mu) = 0$. This equation is formally analogous to the equation of baryon-number conservation (22), where the baryon number is replaced with the entropy: it expresses entropy conservation.

- (5) (B.4) gives $Dn/n = -\partial_\mu u^\mu$. Similarly, the equation of entropy conservation gives $Ds/s = -\partial_\mu u^\mu$. It follows that $D(s/n) = (s/n)(Ds/s - Dn/n) = 0$. This equation means that the entropy per baryon, s/n , is constant along a comoving fluid element.

- (6) Again, write the equation of energy–momentum conservation as the sum of three terms:

$$(\epsilon + P)u^\mu \partial_\mu u^\nu + \partial_\mu((\epsilon + P)u^\mu)u^\nu - \partial^\nu P = 0. \quad (\text{B.6})$$

Multiply by $\Delta_{\rho\nu}$, then the second term disappears and $\Delta_{\rho\nu}\partial_\mu u^\nu = \partial_\mu u_\rho$. One thus obtains immediately

$$(\epsilon + P)Du_\rho = \Delta_{\rho\nu}\partial^\nu P. \quad (\text{B.7})$$

In the nonrelativistic limit, $\Delta_{\rho\nu}$ projects onto the space components, so that $\Delta_{\rho\nu}\partial^\nu P$ is the pressure gradient. $\epsilon + P$ reduces to the mass density and one recovers Euler's equation, i.e., Newton's second law of motion applied to the fluid element.

- (7) In Q3 we have projected the equations on the timelike direction u^μ , in Q6 we have projected on space. All the information has been used.

B.2. Solution of problem 2

- (1) The equation for $\rho = 0$ is

$$(\epsilon + P)Du_0 = \Delta_{0\nu}\partial^\nu P. \quad (\text{B.8})$$

For a stationary flow, $\partial^0 P = 0$, and only the spatial components remain on the right-hand side. D reduces to $\vec{u} \cdot \nabla$. Inserting the definition of Δ , one obtains

$$(\epsilon + P)\vec{u} \cdot \vec{\nabla}u_0 = -u_0u_i\partial^i P = -u_0\vec{u} \cdot \vec{\nabla}P. \quad (\text{B.9})$$

Dividing both sides by u_0 , and writing $\vec{u} \cdot \vec{\nabla} = u(d/d\sigma)$, where $d\sigma$ is the length along a streamline, one obtains the result.

- (2) In the nonrelativistic limit, $u_0 \simeq 1 + \vec{v}^2/(2c^2)$: to leading order in \vec{v} , $\ln u_0 = \vec{v}^2/(2c^2)$. Next, $\epsilon + P = \rho c^2$, where ρ is the mass density. For an incompressible fluid, this shows that $v^2/2 + P/\rho$ is a constant along a streamline. This is Bernoulli's equation, which states that when the fluid accelerates, the pressure decreases. This equation has many applications in fluid dynamics; it explains how a tornado can lift objects.
- (3) For a baryonless fluid, (5) and (6) give $dP/(\epsilon + P) = dT/T = d \ln T$. The relativistic Bernoulli equation then becomes $d \ln u^0 + d \ln T = 0$ along a streamline, from which one easily proves the result. The fluid cools as it accelerates.
- (4) $u_0^2 - u^2 = 1$, hence $u_0 du_0 = u du$. This implies $du/u = (du_0/u_0)/v^2$. We then write $dP = c_s^2 d\epsilon$ (33), and $d\epsilon/(\epsilon + P) = ds/s$ (10). This gives the result.
- (5) Conservation of entropy implies that the entropy flux is constant along the flux tube. This implies that $su\Sigma$ is constant. In differential form, this writes

$$\frac{ds}{s} + \frac{du}{u} + \frac{d\Sigma}{\Sigma} = 0. \quad (\text{B.10})$$

- (6) Replacing du/u with the result of Q4 in the above equation gives the result. If the streamlines diverge, $d\Sigma/\Sigma$ is positive. For a supersonic flow, $v > c_s$, this implies $ds > 0$, i.e., the density decreases along the streamline. For a subsonic flow, it increases.
- (7) For a gas expanding into the vacuum, streamlines obviously diverge, and the density decreases. This means that the flow is supersonic. As the fluid cools, it accelerates, $u_0 \propto 1/T$. As the fluid becomes cooler and cooler, the mean free path becomes eventually too large for hydro to be valid. This occurs when the flow is ultrarelativistic, i.e., $u^0 \gg 1$. In the nonrelativistic case, this condition becomes $v \gg c_s$, and this is called 'hypersonic flow'.

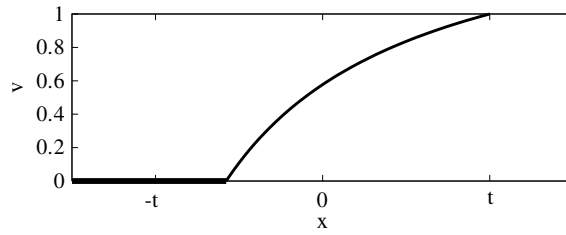


Figure B1. Velocity profile for the Riemann problem.

B.3. Solution of problem 3

- (1) One expects the matter to flow to the right, so that the density will smoothly decrease as a function of x . Since the information cannot propagate faster than the speed of light, one expects that the density is ϵ_0 for $x < -t$ and 0 for $x > t$. The flow occurs in the interval $-t < x < t$.
- (2) One simply does the replacements $\partial/\partial x = (1/t) d/d\zeta$, $\partial/\partial t = -(\zeta/t) d/d\zeta$. The system of equations becomes

$$-\zeta \frac{d\epsilon}{d\zeta} + (\epsilon + P) \frac{dv}{d\zeta} = 0 \quad \frac{dP}{d\zeta} - \zeta(\epsilon + P) \frac{dv}{d\zeta} = 0. \quad (\text{B.11})$$

- (3) Replacing dP with $c_s^2 d\epsilon$, one obtains a linear system of two equations with unknowns $d\epsilon/d\zeta$ and $dv/d\zeta$. The system has a trivial solution $dv/d\zeta = d\epsilon/d\zeta = 0$. It has non-trivial solutions only if the determinant vanishes, which gives $\zeta^2 = c_s^2$, i.e. $\zeta = \pm c_s$. The conditions $d\epsilon/d\zeta < 0$ and $dv/d\zeta > 0$ imply $\zeta < 0$ (see the equations above). The correct solution is therefore $\zeta = -c_s$. The matter starts to flow at $x = -c_s t$. For $x < -c_s t$, the flow velocity is 0 and the density is equal to the initial value ϵ_0 , corresponding to the trivial solutions of the hydrodynamic equations.
- (4) In the frame where the fluid velocity is zero, $\zeta = -c_s$, which means that the information travels at velocity $-c_s$ with respect to the fluid. Under a Lorentz boost of velocity v , the relativistic addition of velocities applies, so that $\zeta = (v - c_s)/(1 - v c_s)$.
- (5) Inverting the relation, we obtain $v = (\zeta + c_s)/(1 + \zeta c_s)$. The maximum value of v is 1, which corresponds to $\zeta = 1$. Note that the fluid velocity at $x = 0$ is exactly c_s . The velocity profile is shown in figure B1.

References

- [1] Landau L D 1953 *Izv. Akad. Nauk Ser. Fiz.* **17** 51
- [2] Ackermann K H *et al* (STAR Collaboration) 2001 *Phys. Rev. Lett.* **86** 402
- [3] Landau L D and Lifshitz E M 1959 *Fluid Mechanics (Course of Theoretical Physics vol 6)* (Oxford: Pergamon)
- [4] Huovinen P and Ruuskanen P V 2006 *Ann. Rev. Nucl. Part. Sci.* **56** 163
- [5] Huovinen P 2004 Hydrodynamical description of collective flow *Quark–Gluon Plasma* vol 3, ed R C Hwa and X N Wang (Singapore: World Scientific)
- [6] Kolb P F and Heinz U W 2004 Hydrodynamic description of ultrarelativistic heavy-ion collisions *Quark–Gluon Plasma* vol 3, ed R C Hwa and X N Wang (Singapore: World Scientific)
- [7] Friman B, Baym G and Blaizot J P 1983 *Phys. Lett.* **132B** 291
- [8] Arnold P, Lenaghan J and Moore G D 2003 *J. High Energy Phys.* **JHEP08(2003)002**
- [9] Bjorken J D 1983 *Phys. Rev. D* **27** 140
- [10] Ollitrault J Y 1991 *Phys. Lett. B* **273** 32
- [11] Hirano T, Heinz U W, Kharzeev D, Lacey R and Nara Y 2006 *Phys. Lett. B* **636** 299
- [12] Nonaka C and Bass S A 2007 *Phys. Rev. C* **75** 014902

- [13] Hirano T and Nara Y 2004 *Nucl. Phys. A* **743** 305
- [14] Lappi T and Venugopalan R 2006 *Phys. Rev. C* **74** 054905
- [15] Bearden I G *et al* (BRAHMS Collaboration) 2005 *Phys. Rev. Lett.* **94** 162301
- [16] Eskola K J, Kajantie K and Ruuskanen P V 1998 *Eur. Phys. J. C* **1** 627
- [17] Eskola K J, Ruuskanen P V, Rasanen S S and Tuominen K 2001 *Nucl. Phys. A* **696** 715
- [18] Eskola K J, Honkanen H, Niemi H, Ruuskanen P V and Rasanen S S 2005 *Phys. Rev. C* **72** 044904
- [19] Azimov Y I, Dokshitzer Y L, Khoze V A and Troyan S I 1985 *Z. Phys. C* **27** 65
- [20] Melnitchouk W, Ent R and Keppel C 2005 *Phys. Rep.* **406** 127
- [21] Back B B *et al* (PHOBOS Collaboration) 2002 *Phys. Rev. C* **65** 061901
- [22] Karsch F 2007 *J. Phys. G: Nucl. Part. Phys.* **34** S627
- [23] Fries R J, Muller B, Nonaka C and Bass S A 2003 *Phys. Rev. C* **68** 044902
- [24] Ollitrault J Y 1992 *Phys. Rev. D* **46** 229
- [25] Bhalerao R S, Blaizot J P, Borghini N and Ollitrault J Y 2005 *Phys. Lett. B* **627** 49
- [26] Drescher H J, Dumitru A, Hayashigaki A and Nara Y 2006 *Phys. Rev. C* **74** 044905
- [27] Socolowski O J, Grassi F, Hama Y and Kodama T 2004 *Phys. Rev. Lett.* **93** 182301
- [28] Manly S *et al* (PHOBOS Collaboration) 2006 *Nucl. Phys. A* **774** 523
- [29] Alver B *et al* (PHOBOS Collaboration) 2007 *Phys. Rev. Lett.* **98** 242302
- [30] Cooper F and Frye G 1974 *Phys. Rev. D* **10** 186
- [31] Borghini N and Ollitrault J Y 2006 *Phys. Lett. B* **642** 227
- [32] Adams J *et al* (STAR Collaboration) 2004 *Phys. Rev. Lett.* **92** 112301
- [33] Becattini F and Heinz U W 1997 *Z. Phys. C* **76** 269
Becattini F and Heinz U W 1997 *Z. Phys. C* **76** 578 (erratum)
- [34] Becattini F 1996 *Z. Phys. C* **69** 485
- [35] Lee K S, Heinz U W and Schnedermann E 1990 *Z. Phys. C* **48** 525
- [36] Braun-Munzinger P, Magestro D, Redlich K and Stachel J 2001 *Phys. Lett. B* **518** 41
- [37] Gelis F, Kajantie K and Lappi T 2006 *Phys. Rev. Lett.* **96** 032304
- [38] Huovinen P, Kolb P F, Heinz U W, Ruuskanen P V and Voloshin S A 2001 *Phys. Lett. B* **503** 58
- [39] Adams J *et al* (STAR Collaboration) 2005 *Phys. Rev. C* **72** 014904
- [40] Adams J *et al* (STAR Collaboration) 2004 *Phys. Rev. Lett.* **93** 252301
- [41] Teaney D 2003 *Phys. Rev. C* **68** 034913
- [42] Adler S S *et al* (PHENIX Collaboration) 2003 *Phys. Rev. Lett.* **91** 182301
- [43] Molnar D and Voloshin S A 2003 *Phys. Rev. Lett.* **91** 092301
- [44] Adare A *et al* (PHENIX Collaboration) 2007 *Phys. Rev. Lett.* **98** 162301
- [45] Cercignani C 1988 *The Boltzmann Equation and its Applications* (Berlin: Springer)
- [46] Burnett D 1935 *Proc. Lond. Math. Soc.* **40** 382
- [47] Bhatnagar P L, Gross E P and Krook M 1954 *Phys. Rev.* **94** 511
- [48] Baier R, Romatschke P and Wiedemann U A 2006 *Phys. Rev. C* **73** 064903
- [49] Bhalerao R S and Gupta S 2008 *Phys. Rev. C* **77** 014902
- [50] Meyer H B 2007 *Phys. Rev. D* **76** 101701
- [51] Kovtun P, Son D T and Starinets A O 2005 *Phys. Rev. Lett.* **94** 111601
- [52] Drescher H J, Dumitru A, Gombeaud C and Ollitrault J Y 2007 *Phys. Rev. C* **76** 024905
- [53] Romatschke P and Romatschke U 2007 *Phys. Rev. Lett.* **99** 172301